Electronic and optical properties of cubic SrHfO3 at different pressures: A first principles study

Article *in* Materials Chemistry and Physics · November 2016

DOI: 10.1016/j.matchemphys.2016.11.045

Materials Chemistry and Physics xxx (2016) xxx-xxx

Contents lists available at ScienceDirect

Materials Chemistry and Physics

journal homepage: www.elsevier.com

Electronic and optical properties of cubic $SrHfO_3$ at different pressures: A first principles study

D.P. Rai [a, *], Sandeep [b], A. Shankar [c], Anup Pradhan Sakhya [d], T.P. Sinha [d], B. Merabet [e], M. Musa Saad H.-E [f], R. Khenata [g], Arash Boochani [h], Shahram Solaymani [i], R.K. Thapa [b]

[a] Department of Physics, Pachhunga University College, Aizawl, 796001, India
[b] Department of Physics, Mizoram University, Aizawl, 796009, India
[c] Department of Physics, University of North Bengal, Darjeeling, 734013, India
[d] Department of Physics, Bose Institute, 93/1 Acharya Prafulla Chandra Road, Kolkata, 700009, India
[e] Applied Materials Laboratory, Researchs Center, Sidi Bel Abbes University, 22000, Algeria
[f] Department of Physics, College of Science, Qassim University, Buridah, 51452, Saudi Arabia
[g] Laboratoire de Physique Quantique de la matire et de Modlisation Mathmatique (LPQ3M), Universit de Mascara, Mascara, 29000, Algeria
[h] Department of Physics, Kermanshah Branch, Islamic Azad University, Kermanshah, Iran
[i] Young Researchers and Elite Club, Kermanshah Branch, Islamic Azad University, Kermanshah, Iran

ARTICLE INFO

Article history:
Received 9 May 2016
Received in revised form 20 November 2016
Accepted 23 November 2016
Available online xxx

Keywords:
GGA
Pressure
Bond length
Hybridization
Energy band gap
Dielectric

ABSTRACT

The electronic and optical properties of cubic $SrHfO_3$ under the variation of pressures were investigated by first-principles calculation within the framework of generalized gradient approximation (GGA). The calculated equilibrium lattice constant of cubic $SrHfO_3$ is in good agreement with available experimental and theoretical results. The result shows that $SrHfO_3$ is an insulator with an indirect band gap up to 20.00 GPa, along ($M - \Gamma$). While the application of pressure above 20.00 GPa the band gap changes to direct band gap, along ($\Gamma - \Gamma$). The band gap increases from 3.80 eV to 4.11 eV with the increase in pressure from 0.00 GPa to 35.00 GPa. In order to understand the optical properties of $SrHfO_3$ perovskite, the dielectric function, optical conductivity and electron energy loss are calculated for photon energy up to 14.00 eV. We have also observed the decrease in static dielectric constant with the increase in energy band gap under pressure.

1. Introduction

In the last decades varieties of perovskite materials have been studied theoretically and experimentally [1–4]. ABX_3 (X = F, Cl, I, H, O, etc.) perovskite-type compounds have gained much attention because of their diverse properties and potential technological applications in opto-electronic solid-state devices. Among the perovskite compounds, oxide perovskites (ABO_3) exhibit a variety of interesting physical properties, which can be exploited in a wide range of applications such as optoelectronic, spintronic, thermoelectric, high-dielectric, ferroelectric/piezoelectric and multiferroic materials [5–8], etc. The ideal cubic structure of ABO_3 is simple, with B-O octahedra and the A cations sitting in the space between the octahedra [9,10]. The ABO_3 oxides with direct band gaps (>3 eV) have strong stability against high temperature and strong radiation. Thus the wide band gap ABO_3 oxides are potential candidates for next generation UV photodetectors, vacuum-ultraviolet light emitting (VUVLEDs) devices, due to their multi-coupling property and the multi-freedom manipulating [11,12]. Yoshino et al. has reported that $SrZrO_3$ is suitable for hydrogen absorption thus it may have many potential applications for fuel cells, steam electrolysis and hydrogen gas sensors [13]. On the other hand $SrTiO_3$ is only a room temperature ferroelectric under strain [14]. Moreover earlier studies revealed that $SrHfO_3$ perovskite is a most promising candidate due to their large dielectric constant and sufficient band offsets for electrons and holes which can be use as a gate dielectric material in complementary metal-oxide-semiconductor (CMOS) integrated circuit technology [15–17]. In recent years, there is a tremendous interest in generating the high permittivities by epitaxial growth of perovskite oxides, such as $SrTiO_3$, $BaTiO_3$, etc., on semiconductors [18–20]. Similarly, $SrHfO_3$ films have high-k gate dielectric on Ge, with band offsets (>2 eV) and low leakage current (<105 A/cm^2) at an applied field of 1 MV/cm [21]. Stachiotti et al. studied the cubic phase of $SrHfO_3$ from DFT calculations and reported ferroelectricity due to the temperature-dependent soft mode at zone-center [22]. Many researchers are interested to study the physical properties of deformed perovskite oxides with phase-transitions. In this regard many perovskites were studied and revealed tilt distortion of BO_6 octahedra on treatment with temperature which results in ferroelastic and corresponds to anti-ferrodistortive (AFD) [23–25]. Guennou et al. studied the phase stability of cubic $CaTiO_3$ under pressure and reported the cubic phase stability up to 60 GPa [26]. However most of the perovskites undergoes structural distor-

* Corresponding author.
Email address: dibyaprakashrai@gmail.com (D.P. Rai)

http://dx.doi.org/10.1016/j.matchemphys.2016.11.045
0254-0584/

tions from this parent cubic structure, which can be driven by external parameters such as temperature, pressure, stress etc. While Vali has reported phase transitions of $SrHfO_3$, which can exist in *Pnma(637–873 K), Cmcm(873–1023 K), I4/mcm(1000–1360 K), Pm3m (1360 K <)* phases [27]. As $SrHfO_3$ has an identical crystal structure to $CaTiO_3$/$BaTiO_3$/$SrZrO_3$ [26,28], we can perform the similar investigation. So far, the detailed study of cubic $SrHfO_3$ under pressure have not yet been carried out. As to know the insight of a material's properties for their technological application it is important to understand the structural behavior and inter-atomic bonding under compression. Therefore, we have performed the full potential linearized augmented plane wave (FP-LAPW) method based on density functional calculations to analyze the influence of the pressures' effect on the structural, electronic and optical properties of cubic $SrHfO_3$.

2. Computational details

The primitive cell of $SrHfO_3$ is of cubic structure (space group *Pm3m*) with Hf-O octahedra, cations Sr sitting on the either sides. The unit cell crystal structure of $SrHfO_3$ generated from a 3D visualization program package (VESTA) [29] is presented in Fig. 1. The electronic structures are calculated by adopting the full potential linearized augmented plane wave (FPLAPW) method for KS-DFT, as implemented in the WIEN2K package [30]. The generalized gradient approximation (GGA) is used to describe the electron exchange and correlation. Nonspherical contributions to the charge density and potential within the muffin tin (MT) spheres are considered up to $l_{max} = 10$ (the highest value of angular momentum functions). The cut-off parameter is $R_{MT} \times K_{\max} = 7$ where K_{max} is the maximum value of the reciprocal lattice vector in the plane wave expansion and R_{MT} is the smallest atomic sphere radii of all atomic spheres. In the interstitial region the charge density and potential are expanded as a Fourier series with wave vectors up to $G_{max} = 12$ a.u^{-1}. Brillouin-zone integrations are approximated by using 10000 k-points from Monhkorst Pack scheme [31] which generated 24 × 24 × 24 k-mesh. The number of k-points used in the irreducible part of the Brillouin zone is 286. The criteria for the convergence of the self-consistent DFT calculation is 0.0001 Ry in total energy. Based on Murnaghan' s equation of state [32] volume optimization has been performed to obtain the ground state lattice parameters. The volume versus energy plot is shown in Fig. 1. Our calculated lattice constant is 4.161 Å which is in good agreement with the previous report 4.167 Å [33], 4.114 Å [22], 4.117 Å [34], 4.087 Å [35]. In order to examine the ground state alloying stability of $SrHfO_3$ structure the formation energy (ΔE_f) is calculated at different pressures. The formation energy gives an idea about the existence of stable crystal. Furthermore, the negative values of ΔE_f indicates stronger bonding between the atoms and more alloying stability of the crystal [36]. The energy of formation (ΔE_f) of a compound $SrHfO_3$ is calculated by subtracting the sum of the energies ($E_{Sr} + E_{Hf} + 3E_O$) of pure constituent elements in their stable crystal structures from the total energy (E_f) of the compound. Therefore, the ΔE_f of the compound $SrHfO_3$ is calculated using the following expression [37,38]:

$$\Delta E_f = E_f - \frac{\left(E_{Sr} + E_{Hf} + 3E_O\right)}{(1+1+3)} \quad (1)$$

The calculated formation energy, individual energies of element (Sr, Hf, O) and volume of $SrHfO_3$ under pressure are presented in Table 1.

3. Results and discussions

We have performed the ground state structural relaxation using Murnaghan's equation of state to obtained the optimized lattice parameters. The electronic and optical properties of cubic $SrHfO_3$ was carried out with the optimized lattice constant. An attempt is made to study the effect of compression on the electronic and optical properties. The applied pressure varies from 0.00 GPa to 35.00 GPa, keeping in mind that the cubic structure remain intact. The pressure 0.00 GPa is considered for the ground state stable structure. The application of pressure decreases the volume of the crystal structure as usual, which is shown in Table 1.

3.1. Electronic properties

In this section we have discussed the electronic structure of $SrHfO_3$ at different pressures. The formation and widening of band gap in $SrHfO_3$ with the increase in pressure is a key issue. As we have observed the compression on the system increases the band gap. Our calculated band gap increases from 3.80 eV to 4.11 eV with the application of the pressure (0.00 GPa–35.00 GPa), Table 2. The density of states (DOS) and energy band structures under the applied pressure are given in Figs. 3 and 5, where the E_F coincides with the top of the valence band (O-p). Throughout the calculations the position of the maxima of valence band (VB) remain the same (O-p states). But we have observed the shifting of minima (d-t_{2g}) towards the higher energy range in conduction band (CB) with the application

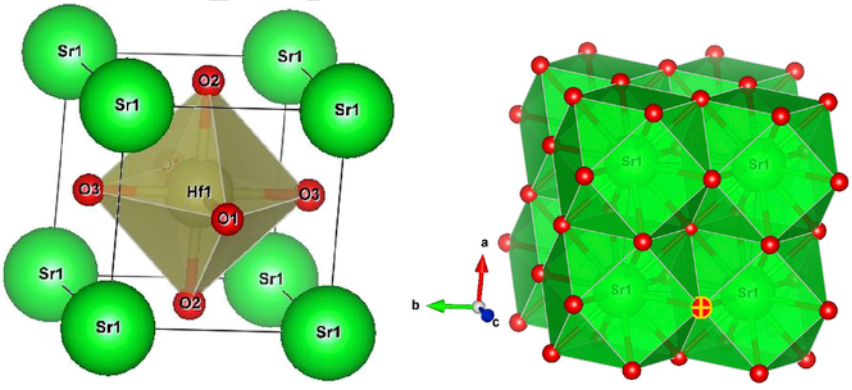

Fig. 1. Unit cell structure of $SrHfO_3$ with Hf-O octahedra.

Table 1
Volume of unit cell, Individual energies (Sr, Hf, O), ΔE_f(Ry), $\Delta H_f = \Delta E_f$/Vol (Ry/a.u.^{3}).

Pressure (GPa)	Volume (a.u.^{3})	Energy (Ry)			ΔE_f(Ry)	ΔH_f(Ry/a.u.^{3})
		Sr	Hf	O		
0.00	486.60	−1685.611	−7952.669	−36.616	−27259.541	−56.020
5.00	474.20	−1685.254	−7951.993	−36.583	−27260.671	−57.488
10.00	466.28	−1685.035	−7951.579	−36.563	−27261.352	−58.466
15.00	455.52	−1684.771	−7951.089	−36.537	−27262.182	−59.845
20.00	449.80	−1684.537	−7950.647	−36.515	−27262.916	−60.612
25.00	445.60	−1684.359	−7950.315	−36.498	−27163.466	−61.184
30.00	438.22	−1684.009	−7949.664	−36.464	−27264.547	−62.202
35.00	431.82	−1683.907	−7949.472	−36.454	−27264.861	−63.140

Table 2
Energy band gap (* sign indicate orthorhombic structure), Static dielectric constant ε_1 (0), Bond length (d_{Sr-O}, d_{Hf-O}).

Pressure (GPa)	Energy gap (eV)		ε_1 (0)	d_{Sr-O} (Å)	d_{Hf-O} (Å)	d_{X-O}(Å) $SrXO_3$ (X = Ru,Hf,Zr,Ti) [13]
	Present	Previous (0.00 GPa)				
0.00	3.800	3.74 [33]	3.625	2.947	2.084	d_{Sr-O} = 2.96 (0.00 GPa)
5.00	3.875	3.60 [46]	3.610	2.914	2.060	d_{Ru-O} = 1.98 (0.00 GPa)
10.00	3.925	3.21 [44]	3.600	2.893	2.046	d_{Hf-O} = 2.06 (0.00 GPa)
15.00	3.975	3.67 [22]	3.585	2.871	2.029	d_{Zr-O} = 2.09 (0.00 GPa)
20.00	4.000	3.20 [47]	3.572	2.850	2.015	d_{Ti-O} = 2.00 (0.00 GPa)
25.00	4.050	3.29 [45]	3.554	2.835	2.005	
30.00	4.100	*6.10 [48]	3.540	2.807	1.985	
35.00	4.110	*6.50 [49]	3.530	2.797	1.978	

of pressure as shown in the inset Fig. 3(a). The Sr-p states have very small contribution near the E_F Fig. 3(b), Sr-p states are grouped at around (12–15) eV in the valence region (not shown in the figure). In general, the opening of the wide band gap in the perovskite is due to the electro-negativity of oxide [39–42]. The oxide perovskite forms the feeble metal-oxide covalent bond. The formation of band gaps are studied on the basis of the bond strength and bond lengths, but with the effect of compression. As reported by Lee et al. the increase in the bond length, decreases the bonding energy as the strength of the covalent bond increases, consequently a smaller band gap [43]. In our calculation we have observed the decrease in the bond lengths for both Sr-O and Hf-O under compression. The calculated bond lengths are in good agreement with the previous results [13], see Table 2. As shown in Figs. (2b–4), the bond length is decreasing while the band gap is increasing with the compression, which is well justified to the findings of Lee et al. The d-t_{2g} orbitals of the transition metal (Hf) ion forms the conduction band minima (CBM) whereas the maximum occupied states in the valence band (VBM) is formed by the anionic O-p orbitals below E_F Fig. 3(c and d). The energy difference between the CBM and VBM leading to the formation of the band gap along the $M - \Gamma$ symmetry, as the pressure increases from 0.00 GPa to 20.00 GPa, Fig. 5(a and b). This gives an indirect band gap which is formed by the charge transfer between O-p and Hf d-t_{2g}. The applied pressure above 20.00 GPa transform the band gap from indirect to direct transition along $\Gamma - \Gamma$ symmetry Fig. 5(c and d). Similar result has also been reported by Feng et al. [44]. The calculated band gaps are in good agreement with the previous theoretical results [22,44–47] and tabulated in Table 2. However the band gap of orthorhombic $SrHfO_3$ determined from x-ray photo-electron spectroscopy experiments are 6.1 eV [48] and 6.5 eV [49] larger than that of cubic $SrHfO_3$. The underestimated band gap from DFT-GGA is as usual as it fails to accounts all the electrons residing in the interstitial region. To get better band gap an orbital independent exchange potential beyond GGA has to be consider within DFT. The cubic $SrHfO_3$ is an insulator by virtue of charge transfer. Though the oxides' electro-negativity is not as high that of halides, the covalent character still prevail and the orbital hybridization between O 2p and Hf-d orbitals occurs [50,51]. The Hf-d orbitals are more extended which results in weaker electron-electron interaction but stronger p-d hybridization effects than those of the 3d transition metal oxides [52]. A report from pseudopotential theory predicts that the hybridization strength is inversely related to bond length (d_{B-O}) [53,54]. This relation states that the decrease in the bond length increases the energy of p-d hybridization. Hence, a significance bond length and the p-d hybridization effect plays an important role in determining the electronic structure of an oxide perovskite. The conduction band is due to the partially occupied or unoccupied states. With the increase in applied pressure the strength of the hybridization increases which enhanced the hybridization between Hf (d-t_{2g}) and O-p electrons which give rise to an antibonding π^* and σ^* bands. The antibonding creates high energy as a result the p-d hybridized bands are pushed up in the energy level away from E_F, subsequently widening the band gap.

3.2. Optical properties

Optical properties, is one of the most important properties of perovskite oxides. The optical properties are in close relation with the band structures of a semiconductor described by the inter-intra band transitions. The intra band transitions are only for metal and neglected, also the contribution of indirect transition is very negligible.

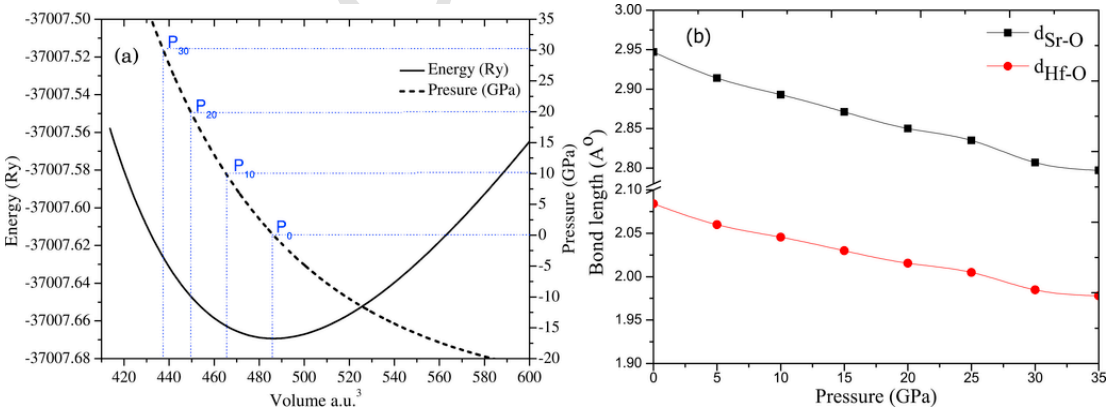

Fig. 2. (a) Energy Vs Volume (Left-Scale) & Pressure Vs Volume (Right-Scale) & (b) Pressure Vs Bond length (Å) (Sr-O, Hf-O).

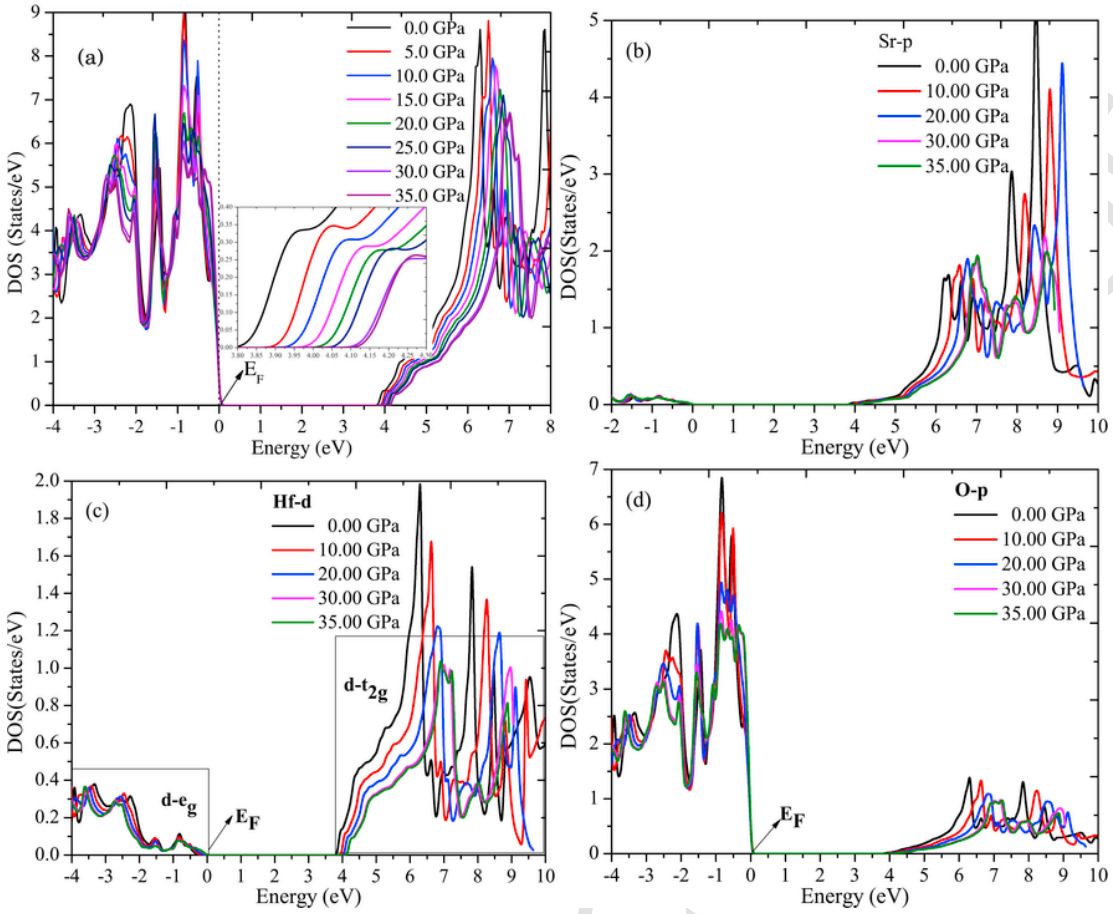

Fig. 3. (a) Total DOS of $SrHfO_3$ under pressure (b) partial DOS, Sr-p under pressure (c) partial DOS, Hf-d under pressure & (d) partial DOS, O-p under pressure.

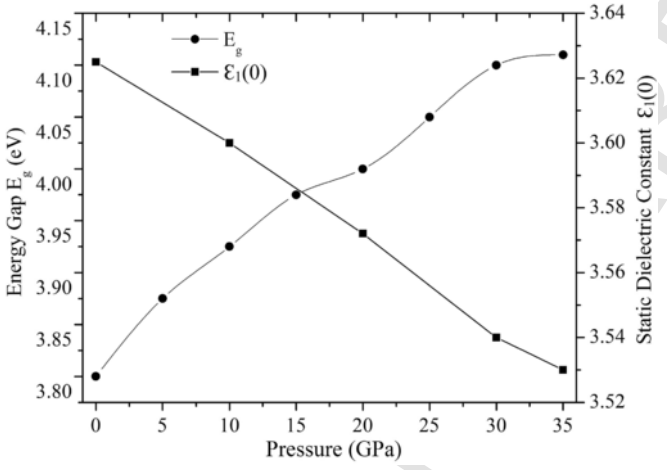

Fig. 4. Variation of Energy Gap under Pressure (Left-Scale) & Variation of Static Dielectric function under Pressure (Right-Scale).

The interaction of the incident photon with the atoms considered as an optical response of a material which can be described by dielectric function, $\varepsilon(\omega)$. For a cubic symmetry structure the crystal is considered to be an isotropic $(\varepsilon = \varepsilon_{xx} = \varepsilon_{yy} = \varepsilon_{zz})$.

Dielectric function $\varepsilon(\omega)$ of the electron gas depending on the frequency has some important role in determining the physical properties of solids. It has two parts real and imaginary [55].

$$\varepsilon = \varepsilon_1(\omega) + i\varepsilon_2 \tag{2}$$

The imaginary part of the complex function ε_2 in cubic symmetry compounds can be calculated by relation [56].

$$\varepsilon_2(\omega) = \frac{8}{2\pi\omega^2}\sum_{nn'}\int_{BZ}\left|Pnn'(k)\right|^2\frac{dS_k}{\nabla\omega_{nn'}(k)} \tag{3}$$

Kramers-Kronig relation gives the real part of the complex dielectric function $\varepsilon_1(\omega)$ [57].

$$\varepsilon_1(\omega) = 1 + \frac{2}{\pi}P\int_0^{\infty}\frac{\omega'\varepsilon_2(\omega')}{\omega'^2 - \omega^2}d\omega' \tag{4}$$

In Equation (3) where $\omega_{nn'}$ is the energy difference between the two states, dS_k is an energy surface with constant value and $P_{nn'}$ is the dipole matrix element between the initial and final states and in Equation (4) P denotes the principal part of the integral. The real part

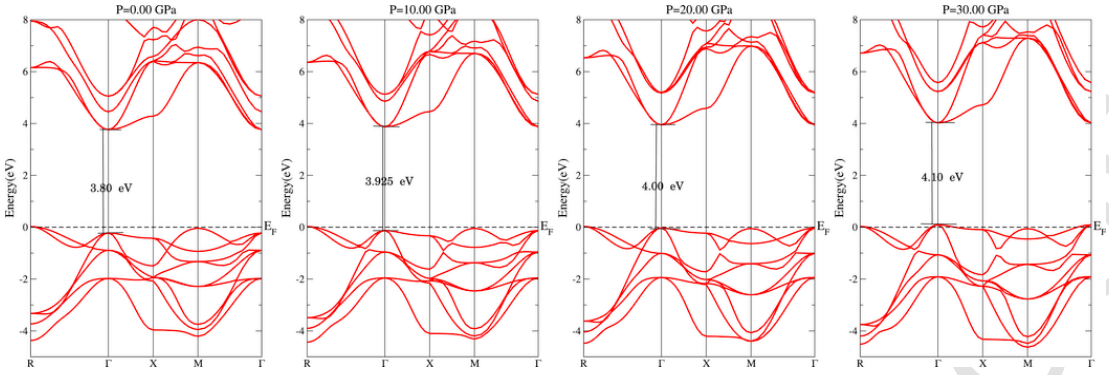

Fig. 5. Band structures of $SrHfO_3$ under Pressure (0.00 GPa, 10.0 GPa, 20.0 GPa, 30.0 GPa).

of the absorption coefficient [58] is

$$\alpha(\omega) = 2\omega k(\omega) = \sqrt{2\omega}\left[\left(\varepsilon_1(\omega)^2 + \varepsilon_2(\omega)^2\right)^{1/2} - \varepsilon_1(\omega)\right]^{1/2} \quad (5)$$

Similarly, the absorption coefficient can be calculated from Beer's law is $\alpha = \frac{2k\omega}{c} = \frac{4\pi k}{c}$. While the electron energy loss function [59] is given by

$$lm\left(\frac{1}{\varepsilon}\right) = -\frac{\varepsilon_2}{\varepsilon_1^2 + \varepsilon_2^2} \quad (6)$$

The static dielectric function $\varepsilon_1(0)$ and low $\varepsilon_1(\omega)$ are strongly dependent on the band gap of the semiconductors. Penn model relating the inverse relation with band gap E_g [60] is

$$\varepsilon_1(0) \cong 1 + \left(\hbar\omega_p/E_g\right)^2 \quad (7)$$

where $(\hbar\omega)$ is the plasma energy. The real dielectric function, imaginary dielectric function, Electron energy loss function (EEL), and Optical conductivity of $SrHfO_3$ is a function of photon energy are presented in Fig. 6(a–d). The real part and imaginary part of the dielectric function can be calculated using the KramersKronig relations [57,61]. With the variation of pressure, $\varepsilon_1(0)$ decreases from 3.625 to 3.530 arb. unit under compression, which represents the dielectric response of a material to a static electric field. This variation in $\varepsilon_1(0)$ is inversely related with the square of the energy gap (E_g) so the higher value of static dielectric constant means low band gap [55]. The calculated value of static dielectric function $\varepsilon_1(0)$ is tabulated in Table 2. Also the variation of $\varepsilon_1(0)$ with pressure is displayed in Fig. 4. The slow rise of $\varepsilon_1(\omega)$ at an energy range 0.0–2.5 eV indicates the interaction of material with the photons. A group of three prominent peaks appear in the range from 3.5 to 4.5 eV. The first sharp peaks at (3.5–12.0) eV is followed by a group of flat peaks at (5.5–6) eV and another group of peaks at (8.5–22.0) eV. After that $\varepsilon_1(\omega)$ becomes negative in the short energy range from 12.00 to 14.00 eV, where the phonon is damped, reaches a minimum and then slowly increases at high energy. Also we have noticed the shifts of the sharp spectral peaks (ε_1) towards the higher energy with increase in pressure, Fig. 6(a).The imaginary part is related to the band structure and describes the absorptive behavior. Fig. 6(b) shows the imaginary part of dielectric function, the optical response occurs at approximately 3.2 eV, representing the threshold value for direct optical transition from VB (O-p) to CB Hf (d-t_{2g}) which may be considered along $\Gamma - \Gamma$ point at 0.00 GPa, Fig. 5(a). After this point, the $\varepsilon_2(\omega)$ spectral lines rapidly increases because of the abrupt increase in the number of transitions followed by a sharp and a flat peak. The peak occurs at 5.8 eV, originated from the transition along $\Gamma - \Gamma$ point, and the second peak with low amplitude occurs at 9.3 eV, which is possibly from direct transitions along $M - M$ point, Fig. 5(a). After calculating the imaginary and real parts of the dielectric function, the optical absorption coefficient $\alpha(\omega)$ and energy loss function (EEL) were calculated. Fig. 6(c) represents the graph of electron energy loss (EEL) as a function of photon energy. The EEL is an important parameter to define the non-scattering and elastically scattering of electrons (zero energy loss). At intermediate energies (1.00–14.00 eV) the energy losses are mainly due to the electron excitations. The two prominent group of peaks appear in the energy range (6.00–14.00) eV, the first group of peaks occur at (6.50–9.50) eV and the second group at (11.00–14.00) eV. We have observed that the peaks in the EEL corresponds to the valley in the optical conductivity which indicates the electron scattering at that energy range Fig. 6 (c,d). In Fig. 6(d), the optical absorption peaks shows the strong absorption of the photon energy in the range (3.50–12.00) eV which is in consistent with the $\varepsilon_2(\omega)$. This shows that the compound is optically active within this range (3.5–12.0) eV and can absorb all the UV frequencies.

4. Conclusion

In this present work, the structural, electronic and optical properties of d^0 insulating metal oxides, $SrHfO_3$, with cubic structure is studied using FP-LAPW method. An electronic and optical structures were analyze under compression (pressure). Structural parameters are found to compare well with the available data in the previous reports. A detailed investigation of electronic and optical properties were carried out with increasing applied pressure. We have studied the formation of band gap in cubic $SrHfO_3$ on the basis of p-d hybridization. The cubic $SrHfO_3$ shows indirect band gap up to 20 GPa while it changes to direct band gap above 20 GPa. The widening of the band gap was examine in relation to the atomic bond length with increasing pressure. Our results for the electronic properties of cubic $SrHfO_3$ are shown to agree well with the other theoretical and experimental findings. The dielectric function (real and imaginary part), Electron energy loss function (EEL) and Optical conductivity of $SrHfO_3$ as a function of photon energy are also calculated.

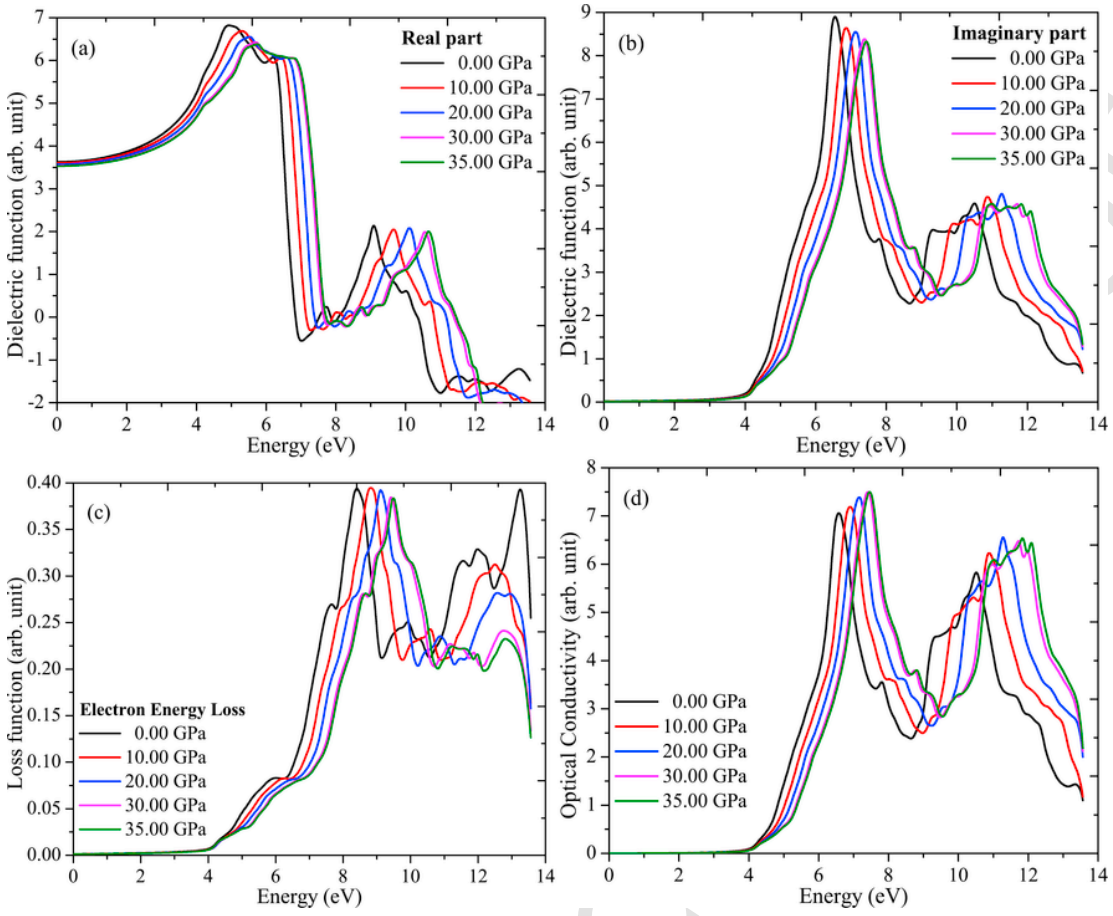

Fig. 6. (a) Real part of Dielectric function (b) Imaginary part of Dielectric function (c) Energy Loss function & (d) Optical Conductivity.

Acknowledgments

D. P. Rai acknowledges UGC Start-Up-Grant No.F.30-52/2014/ BSR (New Delhi, India).

References

[1] J.B. Goodenough, Rep. Prog. Phys. 67 (2004) 1915.
[2] I.A. Leonidov, V.L. Kozhevnikov, E.B. Mitberg, M.V. Patrakeev, V.V. Kharton, F.M.B. Marques, J. Mater. Chem. 11 (2001) 1201.
[3] D.P. Rai, Sandeep, A. Shankar, M.P. Ghimire, R.K. Thapa, Comp. Mater. S. C. 101 (2015) 313–320.
[4] K.Y. Hong, S.H. Kim, Y.J. Heo, Y.U. Kwon, Solid State Commun. 123 (2002) 305.
[5] A.F. Santander Syro, F. Fortuna, C. Bareille, T.C. Rdel, G. Landolt, N.C. Plumb, J.H. Dil, M. Radovi, Nat. Mater. 13 (2014) 1085.
[6] S. Fusil, V. Garcia, A. Barthlmy, M. Bibes, Annu. Rev. Mater. Res. 44 (2014) 91.
[7] M. Bibes, A. Barthlmy, Electron Devices, IEEE Trans. 54 (2007) 1003.
[8] K. Rabe, C. Ahn, J.-M. Triscone, Physics of Ferroelectrics:A Modern Perspective, Springer, Berlin, 2007.
[9] J. Kreisel, B. Noheda, B. Dkhil, Phase Trans. 82 (2009) 633.
[10] A.M. Glazer, Acta Crystallogr. A 31 (1975) 756.
[11] E. Assmann, P. Blaha, R. Laskowski, K. Held, S. Okamoto, G. Sangiovanni, Phys. Rev. Lett. 110 (2013) 078701.
[12] T. Yajima, Y. Hikita, H.Y. Hwang, Nat. Mater. 10 (2011) 198.
[13] Masahito Yoshino, Hiroshi Yukawa, Masahiko Morinaga, Mater. Trans. 45 (2004) 2056–2061.
[14] J.H. Haeni, P. Irvin, W. Chang, R. Uecker, P. Reiche, Y.L. Li, S. Choudhury, W. Tian, M.E. Hawley, B. Craigo, A.K. Tagantsev, X.Q. Pan, S.K. Streiffer, L.Q. Chen, S.W. Kirchoefer, J. Levy, D.G. Schlom, Nature 430 (2014) 758.
[15] J. Robertson, P.W. Peacock, M.D. Towler, R. Needs, Thin Solid Films 411 (2002) 96.
[16] J. Robertson, Rep. Prog. Phys. 69 (2006) 327.
[17] C. Auth, M. Buehler, A. Cappellani, C.-H. Choi, G. Ding, W. Han, S. Joshi, B. McIntyre, M. Prince, P. Ranade, J. Sandford, C. Thomas, Intel. Technol. J. 12 (2008) 77.
[18] R.A. McKee, F.J. Walker, M.F. Chisholm, Phys. Rev. Lett. 81 (1998) 3014.
[19] R. Droopad, Z. Yu, J. Ramdani, L. Hilt, J. Curless, C. Overgaard, J. L.Edwards Jr., J. Finder, K. Eisenbeiser, W. Ooms, Mater. Sci. Eng. B 87 (2001) 292.
[20] A.A. Demkov, A.B. Posadas, H. Seo, M. Choi, K.J. Kormondy, P. Ponath, R.C. Hatch, M.D. McDaniel, T.Q. Ngo, J.G. Ekerdt, ECS Trans. 54 (2013) 255.
[21] M.D. McDaniel, C. Hu, S. Lu, T.Q. Ngo, A. Posadas, A. Jiang, D.J. Smith, E.T. Yu, A.A. Demkov, G. Ekerdt, J. Appl. Phys. 117 (2015) 054101.
[22] M.G. Stachiotti, G. Fabricius, R. Alonso, C.O. Rodriguez, Phys. Rev. B 58 (1998) 8145.
[23] J.F. Scott, Phys. Rev. 183 (1969) 823.
[24] P. Bouvier, J. Kreisel, J. Phys. Cond. Mater. 14 (2002) 3981.
[25] S.A. Hayward, et al., Phys. Rev. B 72 (2005) 054110.
[26] M. Guennou, P. Bouvier, B. Krikler, J. Kreisel, Phys. Rev. B 82 (2010) 134101.
[27] R. Vali, Solid State Commun. 149 (2009) 519.
[28] S.L. Wei, D.Y. Feng, Y.X. Qing, Q.L. Xia, Chin. Phys. Lett. 27 (2010) 096201.
[29] K. Momma, F. Izumi, J. Appl. Crystallogr. 44 (2011) 1272–1276.
[30] P. Blaha, K. Schwarz, G.K.H. Madsen, D. Kvasnicka, J. Luitz, K. Schwarz, An Augmented PlaneWave + Local Orbitals Program for Calculating Crystal Properties Revised Edition WIEN2k 13.1 (Release 06/26/2013), 3, Wien2K Users Guide, 2008. 9501031–1-2.
[31] H.J. Monkhorst, J.D. Pack, Phys. Rev. B 13 (1976) 5188.
[32] F.D. Murnaghan, Proc. Natl. Acad. Sci. U. S. A. 30 (1944) 244.
[33] Z.F. Hou, Phys. Status Solidi B 246 (2009) 135139.
[34] B.J. Kennedy, C.J. Howard, B.C. Chakoumakos, Phys. Rev. B 60 (1999) 2972.

[35] P. Narchuk, M. Kovba, V. Levitskii, Dokl. Phys. Chem. 256 (1981) 11.
[36] N.A. Zarkevich, T.L. Tan, D.D. Johnson, Phys. Rev. B 75 (2007) 104203.
[37] A. Yakoubi, O. Baraka, B. Bouhafs, Results Phys. 2 (2012) 58–65.
[38] D.P. Rai, A. Shankar, Sandeep, M.P. Ghimire, R. Khenata, R.K. Thapa, RSC Adv. 6 (2016) 13358.
[39] K.E. Babu, N. Murali, K.V. Babu, P.T. Shibeshi, V. Veeraiah, Acta Phys. Pol. A 125 (2014) 1179–1185.
[40] T. Fukuda, K. Shimamura, A. Yoshikawa, E.G. Villora, Opto-Electron. Rev. 9 (2011) 109–116.
[41] M. Harmel, H. Khachai, A. Haddou, R. Khenata, G. Murtaza, B. Abbar, S. Bin Omran, M. Khalfa, Acta Phys. Pol. A 128 (2015) 34–42.
[42] A. Duvel, S.E. Wegner, K. Efimov, A. Feldhoff, P. Heitjans, M. Wilkening, J. Mater. Chem. 21 (2011) 6238.
[43] J.S. Lee, Y.S. Lee, T.W. Noh, Phys. Rev. B 70 (2004) 085103.
[44] L.P. Feng, Z.Q. Wang, Q.L. Liu, T.T. Tan, Z.T. Liu, Chin. Phys. Lett. 29 (2012) 127103.
[45] Q.J. Liu, Z.T. Liu, C.P. Feng, T. Hao, Commun. Theor. Phys. 54 (2010) 908–912.
[46] Y.X. Wang, C.L. Wang, W.L. Zhong, J. Phys. Chem. B 109 (2005) 12909.
[47] X. Yu, X.G. Luo, G.F. Chen, J. Shen, Y.X. Li, Acta Phys. Sin. 56 (2007) 5366.
[48] G. Lupina, G. Kozowski, J. Dabrowski, P. Dudek, G. Lippert, H.J. Mssig, Appl. Phys. Lett. 93 (2008) 252907.
[49] D.J. Lee, Y.K. Seo, Y.S. Lee, H.-J. Noh, Solid State Commun. 150 (2010) 301.
[50] J. Okamoto, T. Mizokawa, A. Fujimori, Phys. Rev. B 60 (1999) 2281.
[51] D. Singh, J. Appl. Phys. 79 (1996) 4818.
[52] H.J. Noh, B.J. Kim, S.J. Oh, J.H. Park, H. Lin, C.T. Chen, Y.S. Lee, K. Yamaura, E.T. Muromachi, J. Phys. Condens. Matter. 20 (2008) 485208.
[53] W. A. Harrison, Electronic Structure and Physical Properties of Solids (Freeman, San Francisco, 1980).
[54] M. Imada, A. Fujimori, Y. Tokura, Rev. Mod. Phys. 70 (1998) 1039.
[55] I. Ajmad, B. amin, M. Maqbool, S. Muhammad, G. Murtaza, S. Ali, A. Noor, Chin. Phys. Lett. 29 (2012) 097102.
[56] B. Amin, I. Ahmad, M. Maqbool, S. Goumrisaid, R. Ahmad, J. Appl. Phys. 109 (2011) 023109.
[57] F. Wooten, Optical Properties of Solids, Academic Press New York, 1972.
[58] M. Fox, Optical Properties of Solids, Oxford University Press, Oxford, 2001.
[59] P.H. Mott, J.R. Dorgan, C.M. Roland, J. Sound Vib. 312 (2008) 572575.
[60] D. Penn, Phys. Rev. B 128 (1962) 2093.
[61] D.P. Rai, M.P. ghimire, R.K. Thapa, Semiconductors 48 (2014) 1447–1457.